The 10th JFPS International Symposium on Fluid Power FUKUOKA 2017 Oct. 24-27, 2017 JFPS The Japan Fluid Power System Society

SENSORLESS POSITION CONTROL OF DIRECT DRIVEN HYDRAULIC ACTUATORS

Tom Sourander, Matti Pietola, Tatiana Minav, Henri Hänninen

*Department of Mechanical Engineering, Aalto University School of Engineering
Espoo, Finland
(E-mail: tom.sourander@aalto.fi)

Abstract. This study investigates sensorless position control of valveless pump-controlled hydraulic actuators for non-road mobile machinery (NRMM). The utilized hydraulic systems are direct driven hydraulics (DDH), a type of electrohydrostatic actuators (EHA), which uses an electric servomotor to drive hydraulic pumps of a single actuator. The advantages of DDH over traditional valve-controlled hydraulics are increased energy efficiency due to elimination of the valve losses and improved controllability. The servomotor driven pumps provides a possibility for sensorless position control of hydraulic cylinders without need for sensors. The sensorless position control was realized by simulating the interaction of DDH units and hydraulic cylinders of a testbed prototype hybrid mining loader. Measured data from a test work cycle was used to test the accuracy of the simulation. The results demonstrated that accuracy with maximum error of about 30 mm could be achieved with no load and with 1040 kg load.

Keywords: Sensorless position control, Virtual sensors, Direct driven hydraulics, Electrohydrostatic actuator

INTRODUCTION

In efforts to reduce operating costs and harmful emissions of hydraulic machinery, there has been increasing research to find solutions for replacing and improving conventional systems. In non-road mobile machinery (NRMM), hybrid and electric powertrains have gained popularity due to the high efficiency of electric industrial motors. In hydraulic systems, electric motors have generally been utilized to drive pumps for conventional valve-controlled systems that suffer from throttling losses.

To replace valve-controlled systems, electric servomotor driven pump-controlled systems have been increasingly researched. Pump-controlled systems that operate a single actuator are generally called electro-hydrostatic actuators (EHA). In this study, a variation of EHA, direct driven hydraulics (DDH) is utilized. The advantages of DDH over traditional valve-controlled systems is mainly increased energy efficiency from elimination of valve throttling and idling losses as well as reduced oil cooling requirements. Direct pump control by servomotor provides improved and efficient actuator control with no need for servovalves. The most typical problem with EHA-like systems is caused by the difference in the volume between piston and rod sides in single-rod cylinders and thus the required flow rate ratio. This has been commonly solved by using double-rod symmetrical cylinders, however, this solution requires more space [1]. Solutions for single-rod cylinders involve pilot operated check-valves that compensate for the flow difference or separate pumps for either side that ideally have the same displacement ratio as the cylinder [1, 2].

With a trend of energy efficient machinery becoming more automatized, implementation of advanced control technologies and increased utilization of various sensors is required. Several common types of internal and external cylinder position sensors exist with their advantages and disadvantages [3]. However, these sensors can be expensive and challenging to utilize in applications that require reliability in harsh environments. Therefore, measuring the cylinder position with indirect means has gained research interest. Sensor virtualization is becoming more researched and utilized in various industrial applications, for example, car window DC motor [4] and steel sheet rolling mill [5]. With DDH, it is possible to realize sensorless position control of hydraulic cylinders by utilizing only torque and rotational speed data of the servomotor while accounting errors caused by hydraulic leakage loss.

Indirect position estimation of DDH actuated cylinders has been previously researched in Aalto University. In [6] the position estimation of a DDH actuated cylinder was studied by measuring the pump leakage in the locked position and calculating a slip coefficient that accounted for all leakages. In [7] sensorless position control in an electro-hydraulic forklift was researched. The position estimation in these studies was based on measurements and temperature changes were not accounted and also constant pump efficiencies was assumed. The results in both research showed error in the range of 1-3 % during lifting and lowering. Also in [6], accumulation of error was observed in repeated lifting-lowering cycles due to inaccuracy in pressure estimation.

As a part of project El-Zon, sensorless position control of DDH actuated cylinders is investigated based on simulation of DDH units installed into a testbed prototype mining loader [8]. The cylinder position calculation method is based on Matlab/Simulink simulation model of the DDH units [9]. In the study described in [9] the position calculation accuracy was tested by comparing the calculated cylinder position to the actual position within the simulation. The research of this paper utilizes measurement data of the real DDH units to test the accuracy of the sensorless position algorithm in test work cycles. The following section describes the test setup followed by results of test measurements and finally conclusion and discussion.

DESCRIPTION OF TEST SETUP

The test platform for the DDH units is a prototype mining loader that has been converted to diesel-electric serial hybrid. The front section consists of a boom and bucket. The boom is actuated by two parallel cylinders and the bucket by one cylinder. The bucket cylinder is attached to a linkage mechanism that keeps the bucket angle stationary during the lifting of the boom. The loader has two DDH units, which drive the boom and bucket cylinders. Figure 1 presents a simplified model of the boom and bucket mechanism of the mining loader. Table 1 presents dimensions and utilized parameters of the boom and bucket cylinders of the loader. Here, A-side to the piston side and B-side to the rod side of the cylinder. Cylinder frictions were based on previous measurements with smaller cylinders [10] and linearly scaled up to the loader cylinder dimensions [9].

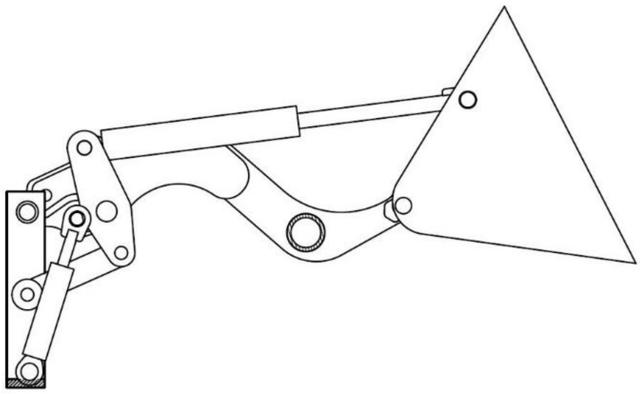

FIGURE 1. Simplified model section of the loader boom and bucket. [9]

TABLE 1. Parameters of the boom and bucket cylinders of the loader.

Parameter	Boom cylinder	Bucket cylinder
Stroke (mm)	311.15	850
A-side area (mm^2)	10261	18050
B-side area (mm^2)	7096.9	11847
Area ratio	1.446	1.524
Static friction (N)	570	760
Coulomb friction (N)	170	220
Viscous friction (N)	41000	41000

The DDH units were dimensioned to provide similar movement speed performance as the original system and the displacement ratio of the A- and B-side pumps was chosen to be as close as possible to the cylinder area ratios. The DDH units consist of an electric motor, motor controller, internal gear pumps [11], belt reduction transmission to better adjust the displacement ratios, pressure relief valves, anti-cavitation valves, cylinder safety valves and oil reservoir. Figure 2 presents a hydraulic diagram and the components of the boom DDH unit. The bucket unit is identical with the exception of different size pumps and a single cylinder. Data acquisition consists of the pressure, the oil temperature and draw-wire cylinder distance sensors. The motor is powered by a 60 Ah, 96V lithium-titanate battery pack [12]. Table 2 presents relevant parameters of the pumps.

Control network for the motor controllers and sensors is implemented utilizing CAN. The control system for the DDH units consist of a main computer unit MicroAutoBox II, which runs a Matlab Simulink-based control software compiled to C++ - code with dSPACE developed CAN toolboxes. This program handles all CAN messages of the sensors, devices and the DDH motor controllers connected to the MicroAutoBox. Graphical monitoring and control of the program is implemented with dSPACE ControlDesk software. The Simulink program also includes data logging features for measurements. The motor controllers can be operated by a joystick or a predetermined test cycle input for more accurate and repeatable control. For testing the accuracy sensorless position control, a realistic test cycle is used, which consist of first lifting the bucket the lifting the boom, dumping and lifting the bucket and finally lowering the boom. The cycles were controlled by PID position controllers with the input being the real cylinder position received from the draw-wire distance sensors and the output the required motor torque. When controlled by the joysticks, the motors are operated in speed control mode.

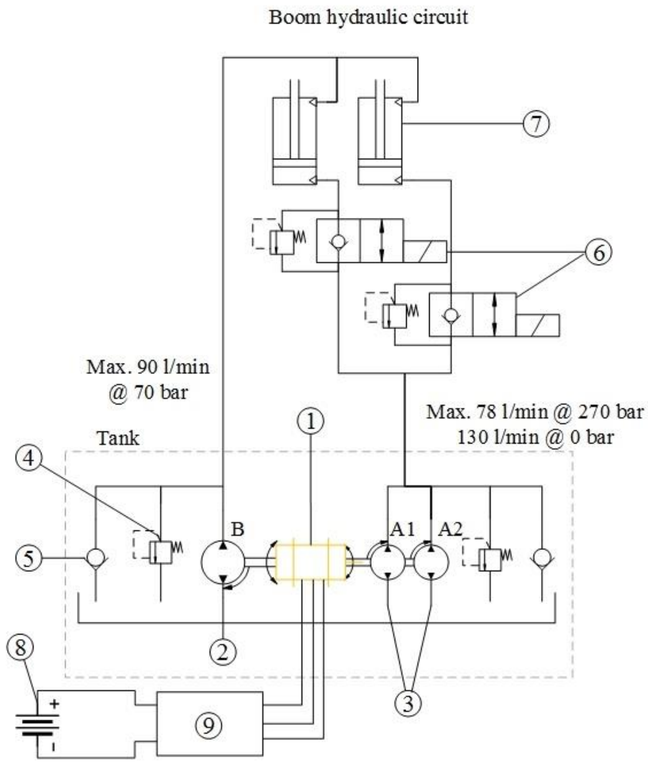

	Component	Model
1	Electric motor	Motenergy ME1304
2	B-side pump	HYDAC PGI100
3	A-side pumps	HYDAC PGI100
4	Pump pressure relief valve	HYDAC DB10P-01
5	Anti-cavitation valve	HYDAC RV12A-01
6	Safety valves	HYDAC WS16ZR-01
7	Hydraulic cylinder	EJC90 original
8	Battery	Altairnano 96 V
9	Motor controller	Sevcon Gen 4 Size 6

FIGURE 2. Hydraulic circuit and components of the boom DDH unit. [9]

Table 2. Parameters of the DDH pumps [11]. Notice that x2 in pump name means that the pumps are double chambered and the displacement in the name is for one chamber and X2 at the end means two parallel pump units, which will work as a single pump unit.

Parameter	**Boom pumps A-side PGI100-008x2 X2**	**Boom pumps B-side PGI100-013+011**	**Bucket pumps A-side PGI100-016x2 X2**	**Bucket pumps B-side PGI100-022x2**
Total displacement (cm^3/rev)	15.8 * 2 = 31.6	24.2	31.6 * 2 = 63.2	44.4
Maximum circuit work pressure (bar)	270	70	70	172
Nominal volumetric efficiency at 250 bar and 1450 rpm	0.93	0.94	0.95	0.95
Nominal hydromechanical efficiency at 250 bar and 1450 rpm	0.91	0.91	0.92	0.93
Maximum rotational speed (rpm)	4200	4000	4000	3600
Gear ratio, motor to pump	28/41	41/47	28/44	44/47
A- and B-side geared flow ratio	1.416		1.542	

The sensorless position control is based on estimation of cylinder piston positions with a simulation model of the bucket arm hydraulic systems [9]. The model was created in Matlab/Simulink using ready-made Simscape fluid power blocks for hydraulics. In the DDH system, the pump speed affects the fluid flow rate and thus the cylinder speed and torque affects the pressure that causes driving force for the cylinder. Multiple sources for non-linearities and errors exist, which is caused by the nature of hydraulics. The most prominent is the volumetric efficiency of the pumps, which affects the leakage flow mainly in function of pressure and oil viscosity. Hydromechanical efficiency of the pump is also important but less significant factor in the total efficiency and error in the produced flow [13]. Other significant affecting factors are the efficiency of the cylinders, bulk compressibility of the oil and pressure losses in the pipelines. These non-linearities make it challenging to calculate the positions of the cylinders. In addition, parameters of some components are based on estimations and simplified calculations as measuring them would be impractical. As the manufacturer of the pumps only provides efficiency curves for nominal operating conditions in which pump speed and oil viscosity are constant [11], it is not possible to directly form efficiency tables for various speed, pressure and temperature conditions. Measuring these was not possible, thus the simulation model calculates pump efficiencies based on Hagen-Poiseuille laminar pipe flow model using the nominal efficiencies as reference points [9]. Due to the pump leakages being mostly pressure dependent, more cylinder load requires higher pump pressure and thus torque, which leads to increased leak flow. This leads to the cylinder movement for a given fluid volume being ultimately dependent on the pump torque, speed and oil viscosity. Thus, it is possible to estimate the movement of a cylinder from the torque and speed of the electric motor. Figure 3 summarizes a diagram of the interaction between different parts and factors related in the sensorless position calculation process.

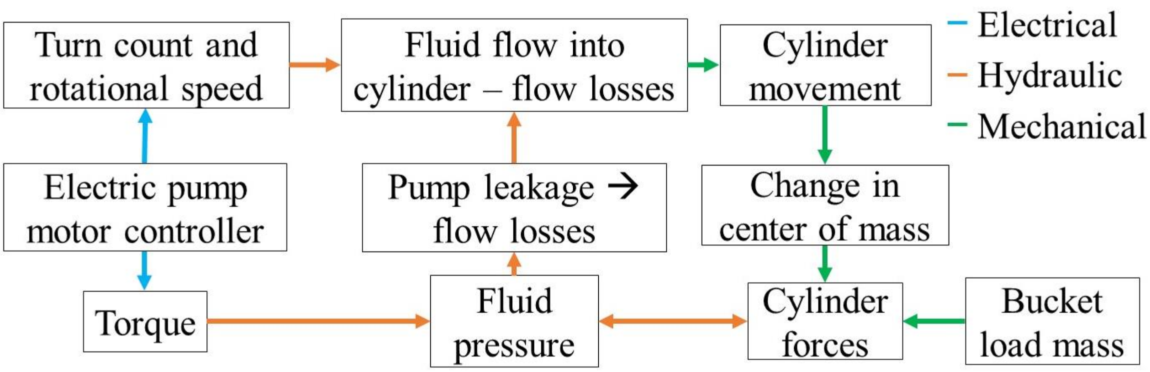

FIGURE 3. Interaction and signals between different parts of the sensorless cylinder position calculation process. [9]

The simulation of the interaction of the motor and the cylinders was performed with cylinder load increasing from a small load to pressure relief valve limit, oil temperature increasing from -5 °C to 100 °C and the motor run at three different speed ranges. The results were saved as lookup tables of cylinder movement in mm per motor revolution in function of motor torque at various temperatures and three motor speed ranges. Since the simulation was run at variable time step, the amount of motor revolutions per step varies. In each time step, the cylinder movement per motor revolution at the current torque is looked up from the tables. This is then compared to the current motor speed to calculate the cylinder movement during the step. The movement at each step is then cumulatively summed to calculate the current cylinder position. For more detailed description of the simulation process, refer to [9].

Figure 4 provides a flowchart explanation of the sensorless control idea of a DDH actuated cylinder. The user in this case is the high-level input source and can be either human or an automated process that provides control inputs to the control software that in turn produces input to the motor controller. The motor controller in turn feeds back torque and speed data from the motor sensors, which are used to calculate the estimated cylinder position. This position data is then fed back into the control software. This way the cylinder position calculation functions as a normal position sensor for the user. In this research, the draw wire position sensor is utilized for the reference positions. In further applications simple proximity sensors, for example Hall-effect, can act as reference points.

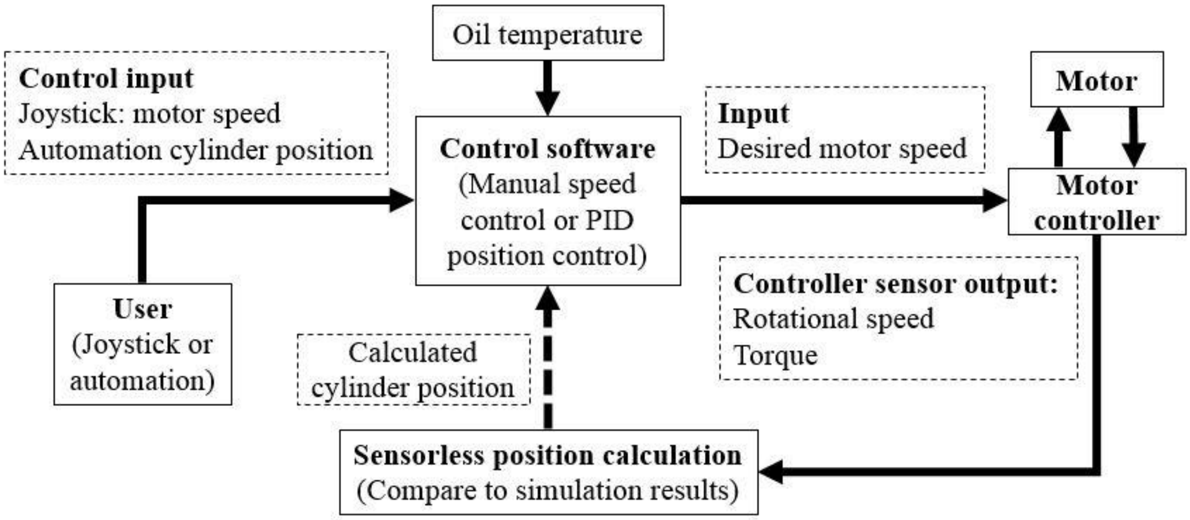

FIGURE 4. Flowchart of the sensorless control method of the DDH cylinders. [9]

RESULTS

First, Figure 5 presents examples of simulation based boom and bucket cylinder movement look-up tables at four different oil temperatures and maximum motor speeds. The bucket motor torque is opposite to the boom due to the bucket cylinder rod-side being the lifting side and thus the motor is driven in negative direction. These figures illustrate that increasing cylinder load and pressure, and thus torque results in less cylinder movement per pump revolution during lifting due to increasing pump leakage and vice versa for lowering. Rapid drop at high torque is caused by the pressure reaching pressure relief valve limit. At higher temperatures, the oil viscosity is lower and thus causing more pump leakage and lower cylinder movement ratio. The sensorless position calculation is based on the lookup tables consisting of these graphs at various temperatures and speeds. The oil temperature during the measurements varied between 25 and 30 °C. The parameters of the oil are based on Shell Tellus T 32 [14], which is VG32 equivalent hydraulic oil.

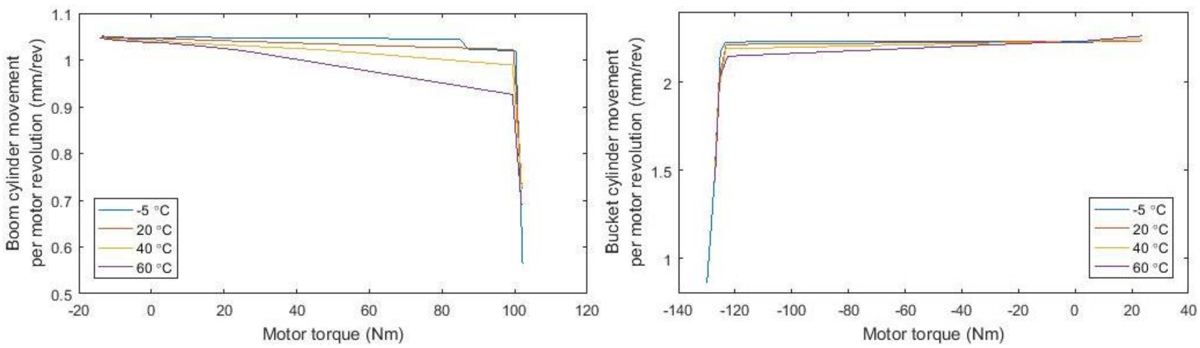

Figure 5. Simulation results: Boom (left) and bucket (right) cylinder movements per motor revolution in function of torque at various temperatures [9].

The measurements were performed by running a lifting-lowering cycle of the boom and bucket at four different speeds and with no load weight at the bucket and with a 1040 kg payload. Results for no load and with load at the highest speed are presented. The maximum speed cycle lasts for about 25 seconds and the motors operate at about 5000 – 6000 rpm.

Figure 6 left part shows the calculated boom cylinder position at no load and maximum cycle speed validated by measurements (marked as real position in the Figure) and the right part shows the error between the measured and calculated values. The calculated positions are as is and are only limited by soft upper and lower limits.

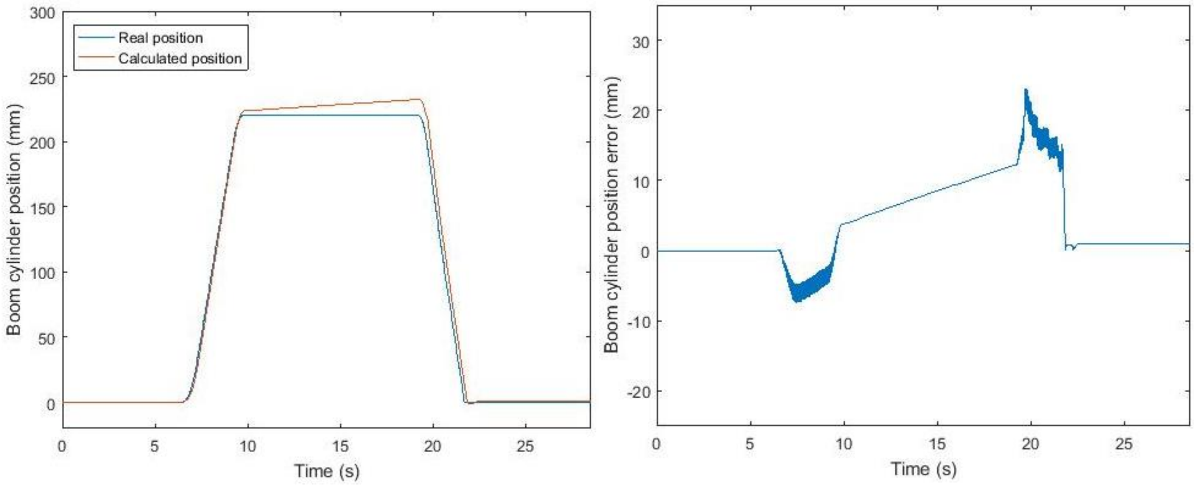

Figure 6. Boom cylinder cycle with no load. Left: Boom cylinder measured real and calculated positions. Right: Difference between the measured real and calculated boom cylinder position.

During the lifting movement, the error accumulation is minimal and is apparently mainly caused by the beginning acceleration and end deceleration. When the cylinder real position has reached the top position, the calculated position continues to creep upwards. This is can be explained as the boom motor maintains a speed of about 60 rpm (Figure 7), which does not affect the cylinder speed however it manages to deceive the position calculator. This is ultimately caused by low accuracy PID control to achieve smoother movement. Faster responding PID would result in better accuracy at the cost of sharp torque spikes and motor speed oscillation, which are detrimental to the position calculator.

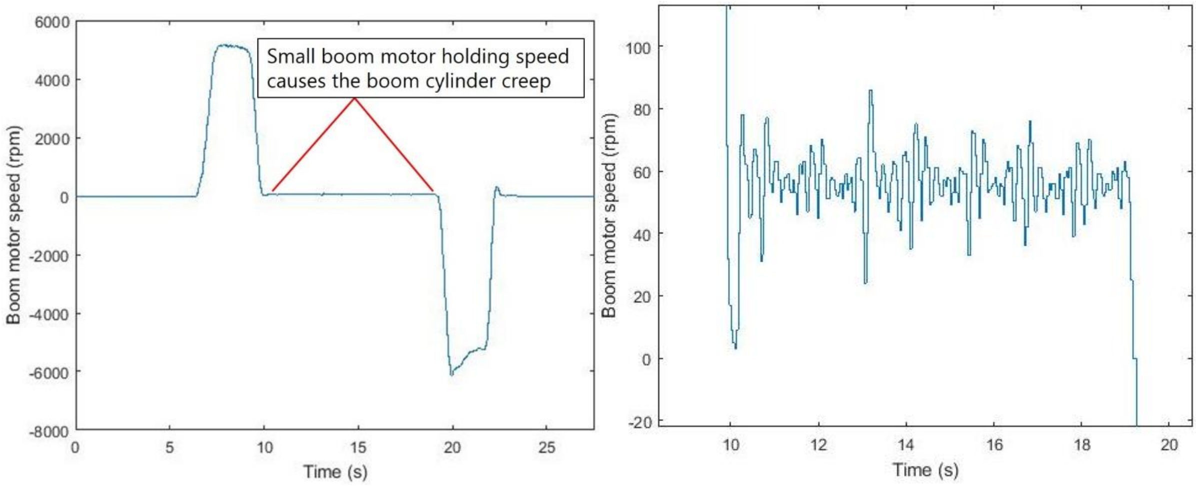

Figure 7. Left: Boom motor speed at maximum cycle speed. Right: Zoom of the error causing motor creep speed.

Figure 8 left part presents the measured and calculated positions of the bucket cylinder during the same cycle and the right part shows the difference between these.

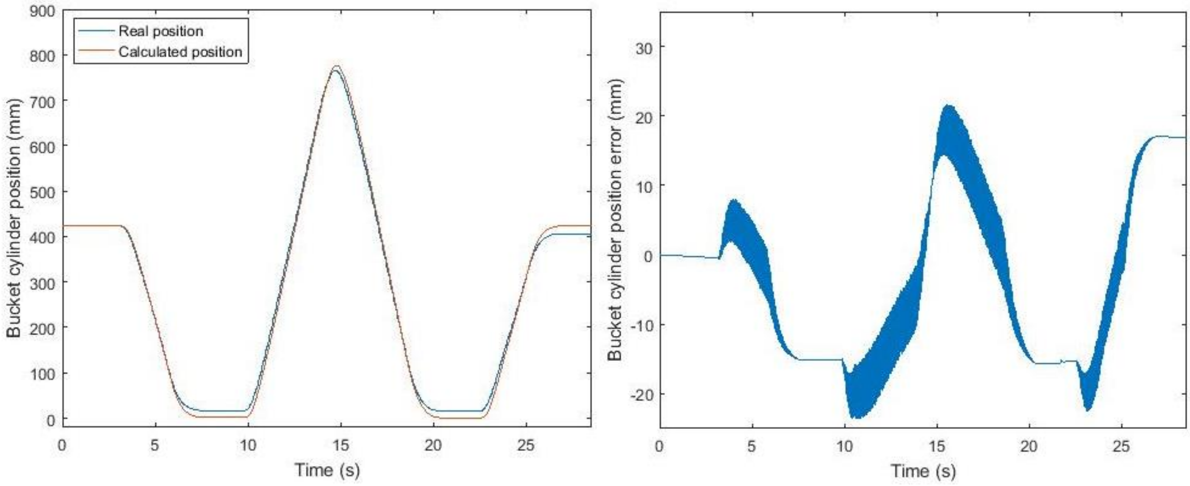

Figure 8. Bucket cylinder cycle with no load. Left: Bucket cylinder measured real and calculated. Right: Difference between the measured real and calculated boom cylinder position.

Figures 9 and 10 present results of the same cycle, however the position calculator now utilizes the end and middle points of the measured position as references. The boom cylinder has a stroke of 311.15 mm so the middle point is rounded to 155 mm. The bucket cylinder middle point is at 425 mm. These movement cycles were not allowed to reach the upper limits due to workspace limitations. In theory, utilizing the reference point compensation should result in less cumulated error over successive cycles.

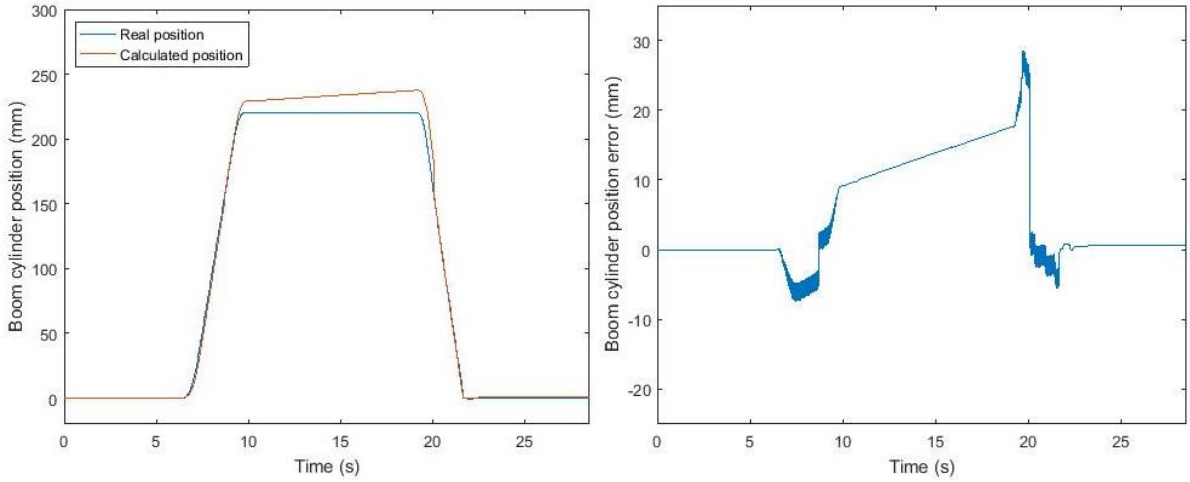

Figure 9. Boom cylinder cycle with reference point compensation and no load. Left: Boom cylinder measured real and calculated positions. Right: Difference between the measured real and calculated boom cylinder position.

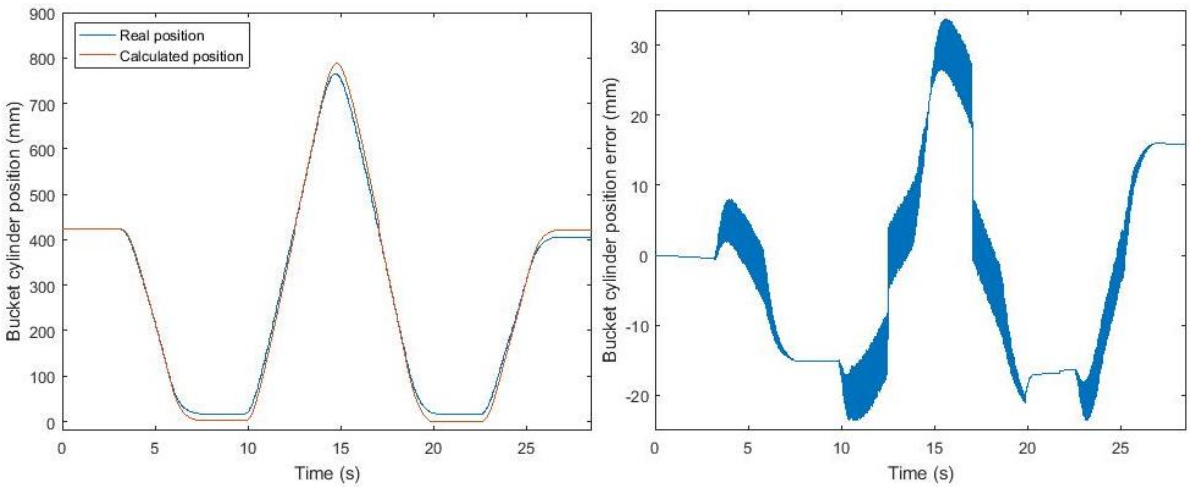

Figure 10. Bucket cylinder cycle with reference point compensation and no load. Left: Bucket cylinder measured real and calculated positions. Right: Difference between the measured real and calculated boom cylinder position.

Figures 11 and 12 presents results for the same cycle performed with a 1040 kg payload attached to the bucket. Figures 13 and 14 add the reference point compensation. The upward creep of the boom cylinder calculated position is also present in these results.

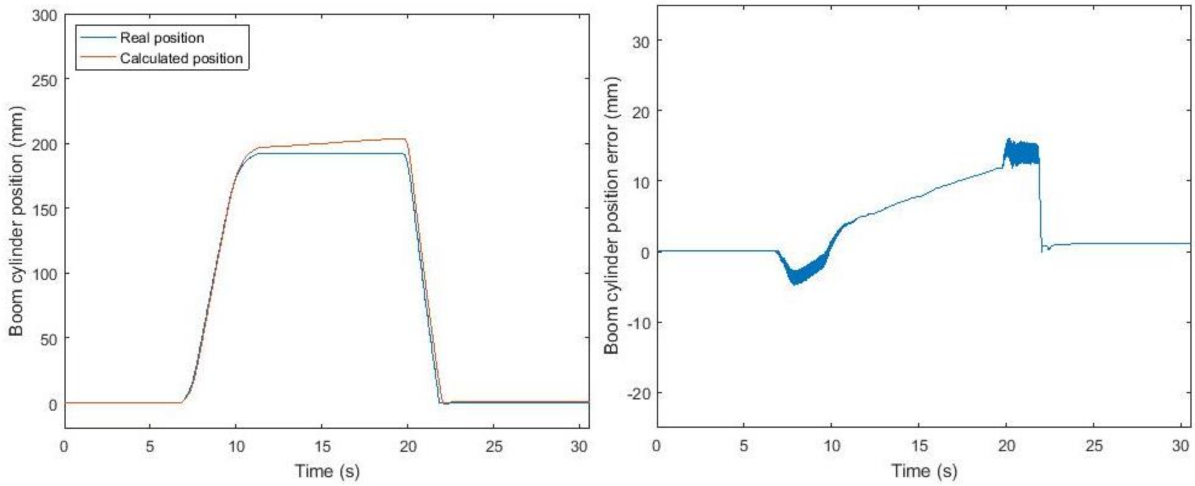

Figure 11. Boom cylinder cycle with a bucket payload of 1040 kg. Left: Boom cylinder measured real and calculated positions. Right: Difference between the measured real and calculated boom cylinder position.

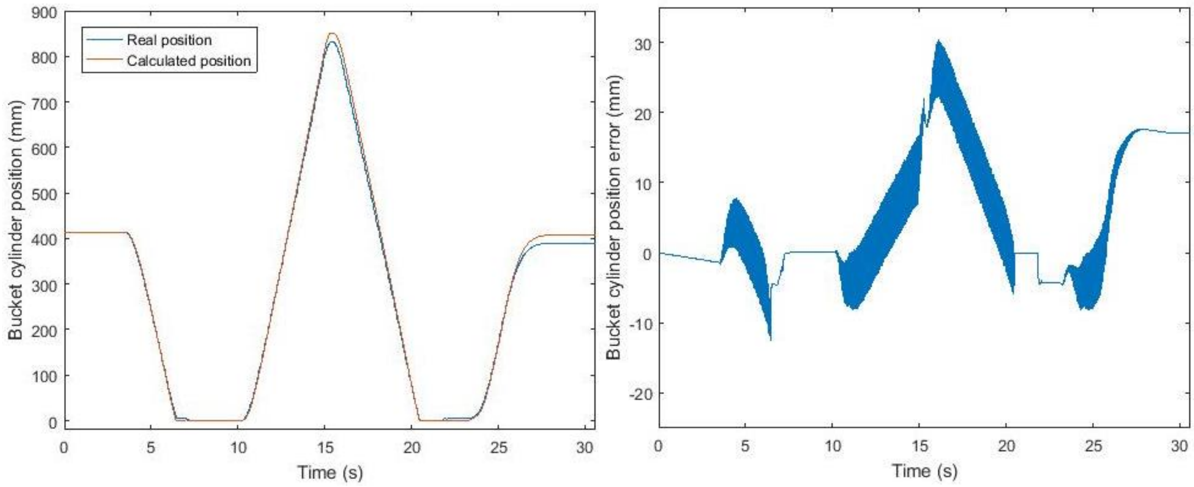

Figure 12. Bucket cylinder cycle with a bucket payload of 1040 kg. Left: Boom cylinder measured real and calculated positions. Right: Difference between the measured real and calculated boom cylinder position.

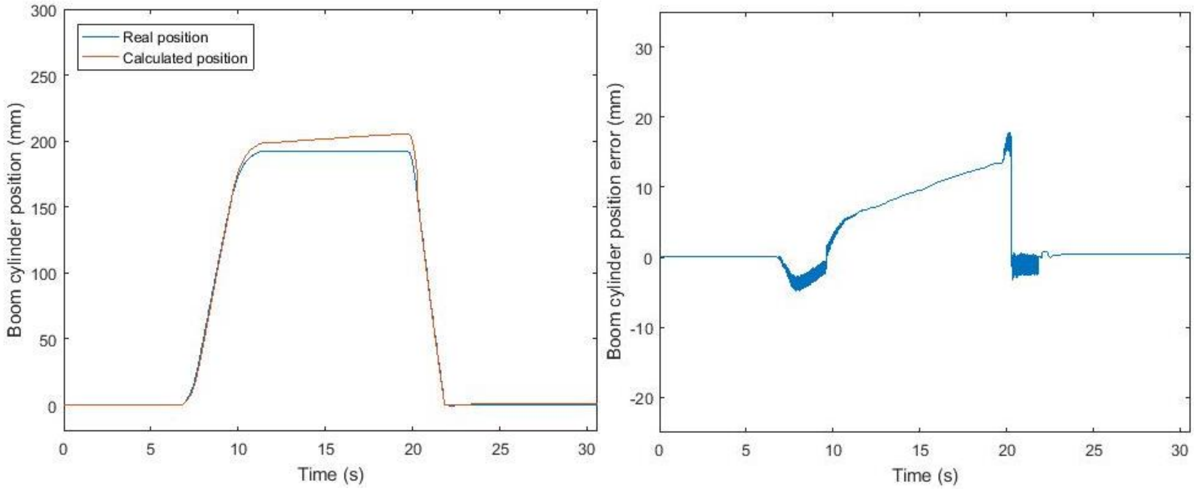

Figure 13. Boom cylinder cycle with reference point compensation and a bucket payload of 1040 kg. Left: Boom cylinder measured real and calculated positions. Right: Difference between the measured real and calculated boom cylinder position.

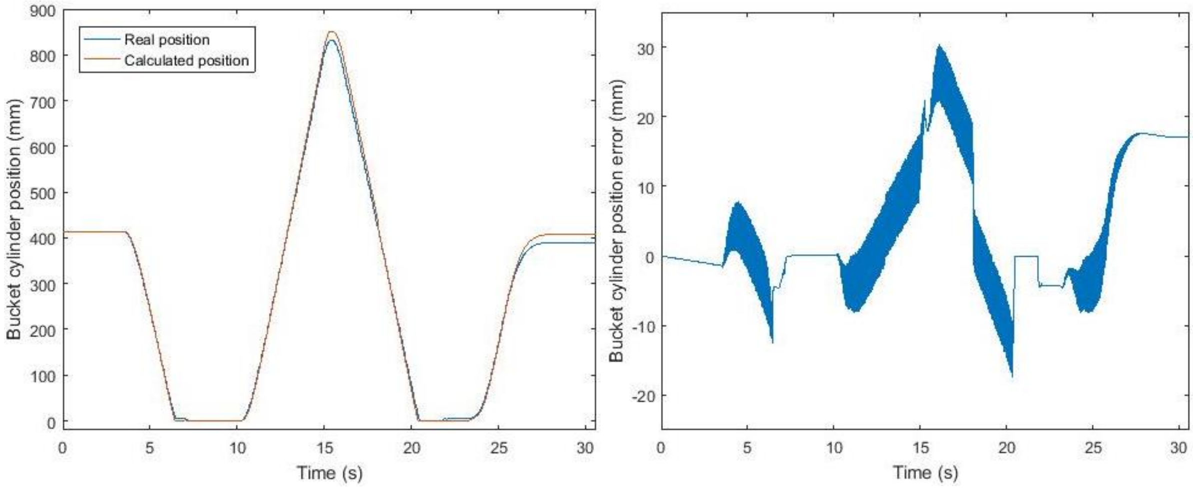

Figure 14. Bucket cylinder cycle with reference point compensation and a bucket payload of 1040 kg. Left: Boom cylinder measured real and calculated positions. Right: Difference between the measured real and calculated boom cylinder position.

Based on the results, the sensorless position calculator manages to achieve an accuracy with the maximum error being about 30 mm. The results demonstrated that the position accuracy is does not vary with payload variation. This accuracy is possibly enough for NRMM applications. The accuracy is slightly worse than in earlier simulation results [9], which could be expected since the hydraulic system in the simulation cannot exactly match the real system.

CONCLUSIONS

This study investigated sensorless position control of valveless pump-controlled hydraulic actuators in an NRMM test platform. The sensorless position control was realized by simulating the hydraulic units and forming look-up tables for the interaction between the cylinder movement and motor torque and speed at various oil temperatures. Measured data from a test work cycle was utilized to test the accuracy of the simulated results. The results demonstrated that accuracy with maximum error of about 30 mm could be achieved with no load and with 1040 kg payload.

The cylinder position calculation still has some limitations. The process is not capable of determining the true start position of the cylinder and will always regard the current starting position as the zero position. While software end limits are implemented, the algorithm is not directly capable of detecting if a cylinder piston has reached an end point. Theoretically, detecting the pressure limit from motor torque is possible however in practice, there can be many situations where the pressure reaches the relief valve limit but the cylinder has not reached an end point. Therefore, reference points at least at the cylinder ends are needed to synchronize the position calculator. Preferably a middle point reference would also be needed since it can be possible that a cylinder is never driven to the end stops. The results show that during a single lift-lower cycle, the reference point compensator does not significantly affect the error and in some cases is able to increase the error. However as mentioned in the previous section, the reference point compensation can help to avoid cumulative error during multiple movement cycles, which improves the average accuracy.

When considering that some simulation parameters of the hydraulic system were based on rough calculations and guesses, the achieved accuracy can be considered sufficient if an error of few centimeters is acceptable for an application. Higher accuracy could be achieved by more thoroughly measuring the relevant parameters and forming a more accurate cylinder movement tables in function of motor torque, speed and oil temperature.

ACKNOWLEDGMENTS

This research was enabled by the financial support of Tekes, the Finnish Funding Agency for Technology and Innovation, (project EL-Zon) and internal funding at the Department of Mechanical Engineering at Aalto University. The cooperation with Lehmuspelto Teemu and Tammisto Otto is highly appreciated.

REFERENCES

1. K. Heybroek. Saving Energy in Construction Machinery using Displacement Control Hydraulics, Concept Realization and Validation. PHD Thesis. Linköping University, Division of Fluid and Mechanical Engineering Systems, Department of Management and Engineering. Lingköping. 2008. 127 p.
2. Manring, N. Hydraulic Control Systems. Hoboken, N.J: John Wiley & Sons, 2005. 446 p. ISBN 0-471-69311-1
3. E. E. Herceg. Taking a Position on Hydraulic Cylinder Sensors. Alliance Sensors Group. Hydraulics & Pneumatics. 2015. Available: http://hydraulicspneumatics.com/cylinders-actuators/taking-position-hydraulic-cylinder-sensors
4. A. Consoli, G. Bottiglieri, R. Letor, R. Ruggeri, A. Testa, S. De Caro. Sensorless Position Control of DC Actuators for Automotive Applications. IAS 2004. MIUR-PRIN 2003: Innovative conversion topologies for electric drives.
5. Pedro, A, Goodwin G. Virtual Sensors for Control Applications. Annual Reviews in Control 26 (2002) 101-112.
6. C. Bonato, T. Minav, P. Sainio, M. Pietola. Position control of direct driven hydraulic drive. Proceedings of the 8th FPNI Ph.D Symposium on Fluid Power, FPNI2014. 2014, June 11-13, 2014, Lappeenranta, Finland
7. T. Minav, L. Laurila, J. Pyrhönen. Relative position control in an electro-hydraulic forklift. International Review of Automatic Control (I.RE.A.CO.), Vol. X, n. X. 2012
8. T. Minav, T. Lehmuspelto, P. Sainio, M. Pietola. Series hybrid Mining loader with zonal hydraulics. 10th International Fluid Power Conference. 2016
9. T. Sourander, M. Pietola, T. Minav, H. Hänninen. Sensorless position estimation of simulated direct driven hydraulic actuators. In: *The 15th Scandinavian International Conference on Fluid Power*, SICFP'17, June 7-9, 2017, Linköping, Sweden.
10. A. Järf. Flow compensation using hydraulic accumulator in direct driven hydraulic differential cylinder application and effects on energy efficiency. Master's thesis. Aalto University, School of Engineering. Espoo 2016. 102 p.
11. Hydac. Medium heavy duty series size 2 PGI100. http://www.hydac.com/fileadmin/pdb/pdf/PRO0000000000000000000002905010012.pdf. Visited on: 1.6.2017
12. Altairnano. 24V 60Ah Battery module. http://www.altairnano.com/products/battery-module/. Visited on: 1.6.2017
13. T. Schimmel. Efficiency of Hydraulic Fluids – Theory and Field Testing. Evonik Oil Additives. Evonik Industries. Helsinki 2013.
14. Shell Lubricants. Shell Tellus oils T Technical datasheet. http://www.epc.shell.com/Docs/GPCDOC_X_cbe_24855_key_140002044283_6623.pdf. Visited on: 1.6.2017

